J Mater Sci (2009) 44:401–407
DOI 10.1007/s10853-008-3145-5

The effect of repeated annealing temperature on the structural, optical, and electrical properties of TiO_2 thin films prepared by dip-coating sol–gel method

O. Pakma · N. Serin · T. Serin

Received: 17 February 2008 / Accepted: 26 November 2008 / Published online: 11 December 2008
© Springer Science+Business Media, LLC 2008

Abstract In this study, we have studied the effect of repeated annealing temperatures on TiO_2 thin films prepared by dip-coating sol–gel method onto the glasses and silicon substrates. The TiO_2 thin films coated samples were repeatedly annealed in the air at temperatures 100, 200, and 300 °C for 5 min period. The dipping processes were repeated 5 to 10 times in order to increase the thickness of the films and then the TiO_2 thin films were annealed at a fixed temperature of 500 °C for 1 h period. The effect of repeated annealing temperature on the TiO_2 thin films prepared on glass substrate were investigated by means of *UV–VIS* spectroscopy, X-ray diffraction (*XRD*), and atomic force microscopy (*AFM*). It was observed that the thickness, average crystallite size, and average grain size of TiO_2 samples decreased with increasing pre-heating temperature. On the other hand, thickness, average crystallite size, and average grain size of TiO_2 films were increased with increasing number of the layer. Al/TiO_2/p-Si metal–insulator–semiconductor (MIS) structures were obtained from the films prepared on p-type single silicon wafer substrate. Capacitance–voltage (*C–V*) and conductance–voltage (G/ω–V) measurements of the prepared MIS structures were conducted at room temperature. Series resistance (R_s) and oxide capacitance (C_{ox}) of each structures were determined by means of the *C–V* curves.

O. Pakma · N. Serin · T. Serin
Department of Engineering Physics, Faculty of Engineering, Ankara University, Tandogan, Ankara 06100, Turkey

O. Pakma (✉)
Department of Physics, Faculty of Arts and Science, Muğla University, Kötekli, Muğla 48000, Turkey
e-mail: pakma@eng.ankara.edu.tr

Introduction

The popularity of such studies on Schottky diodes with native or deposited insulator layer is rooted in their importance in semiconductor technology. In the recent years, insulator layers forming on Si, such as SnO_2 and TiO_2 films, have been examined as a potential material to replace SiO_2. The main advantages of these films are the lower densities of these surface states and their high-dielectric permittivity when compared to SiO_2. The titanium dioxide (TiO_2) has attracted considerable attention for its potential applications in optical components including photocatalysts, optical filters, gas sensors, integrated optical amplifiers, solar cells, and electrochromic displays [1–3]. Various methods have been employed to prepare TiO_2 thin films, for example sputtering [4], e-beam evaporation [5], chemical vapor deposition [6], and sol–gel process [7, 8]. TiO_2 exhibits three crystalline phases (anatase, rutile, and brookite) but its orientations in thin film form depend upon the conditions and parameters of the fabrication method [9, 10]. The sol–gel method is one of the promising methods because optical and other properties of thin films can be controlled easily by changing the solution composition and deposition condition. The film deposition on the substrate can be generally realized by dip-coating and spin-coating techniques.

The metal–insulator–semiconductor (MIS) structure is the most useful device in the study of semiconductor surfaces. Due to the technical significance of MIS structures, these devices have been extensively studied over the past four decades; however, very little experimental information is still available on the barrier formation at insulator–semiconductor interface. The electrical characteristics of these devices do not obey the ideal Schottky theory.

In this paper, it was mainly planned to investigate the effect of repeated annealing temperature on the TiO_2 thin films prepared by sol–gel dip-coating process on glass and silicon wafer substrate and it was aimed to analyze and report its effects on the structural, optical, and electrical properties which will be measured and determined by means of X-ray diffraction (*XRD*), *UV–VIS* spectroscopy, atomic force microcopy (*AFM*), and capacitance–voltage (*C–V*) measurements.

Experimental details

The glass substrates in 1mm × 26 mm × 76 mm dimensions were cleaned by de-ionized water for 30 min in ultrasonic bath and then they were kept in acetone (CH_3COCH_3, Merck) in the ultrasonic bath. Finally they were dried in the furnace 200 °C at for 10 min. A lot of metal–insulator–semiconductor (Al/TiO_2/p-Si) structures were fabricated on the 5 inch diameter float zone <111> p-type (boron-doped) single crystal silicon wafer with a thickness of 600 μm and a resistivity of 5–10 Ωcm. For the fabrication process, Si wafer was degreased through RCA cleaning procedure [i.e., a 10-min boiling in $NH_4OH + H_2O_2 + 6$ DI (18 M Ω de-ionised water), which was followed by a 10-min boiling in $HCl + H_2O_2 + 6$ DI] [11]. Next, it was subjected to the drying process in N_2 atmosphere for a prolonged time. Following the drying process, high-purity aluminium (99.999%) with a thickness of 150 nm was thermally evaporated from the tungsten filament onto the whole back surface of the Si wafer under the pressure of 10^{-7} Torr. In order to obtain a low-resistivity ohmic back contact, Si wafer was sintered at 580 °C for 3 min in N_2 atmosphere. The native oxide on the front surface of the substrate was removed in $HF:H_2O$ (1:10) solution and finally, the wafer was rinsed in de-ionised water for 30 s before forming an organic layer on the p-type Si substrate.

In order to prepare a TiO_2 solution, firstly, 1.2 mL titanium tetraispropoxide [$Ti(OC_3H_7)_4$, Merck] was added to 15 mL ethanol [C_2H_6O, Merck] and the solution was kept in a magnetic stirrer for 1 h. Then, 5 mL of glacial acetic acid [$C_2H_4O_2$, Merck] and 10 mL of ethanol were added to the solution and after each additive component was added, it was mixed in the magnetic stirrer for 1 h. In the final step, 1.5 mL of trietilamine [$(C_2H_5)_3N$, Merck] was added in the solution and the final solution was mixed in the magnetic stirrer for about 3 h. Solution preparation stages are indicated in Fig. 1.

Dipping process was held through homemade motorized system and each sample was dipped for 5 to 10 times. After each dipping process of cleaned glass and p-type silicon crystal into the solution, one substrate of glass and alloy formed surface of Si wafer were cleaned with ethanol.

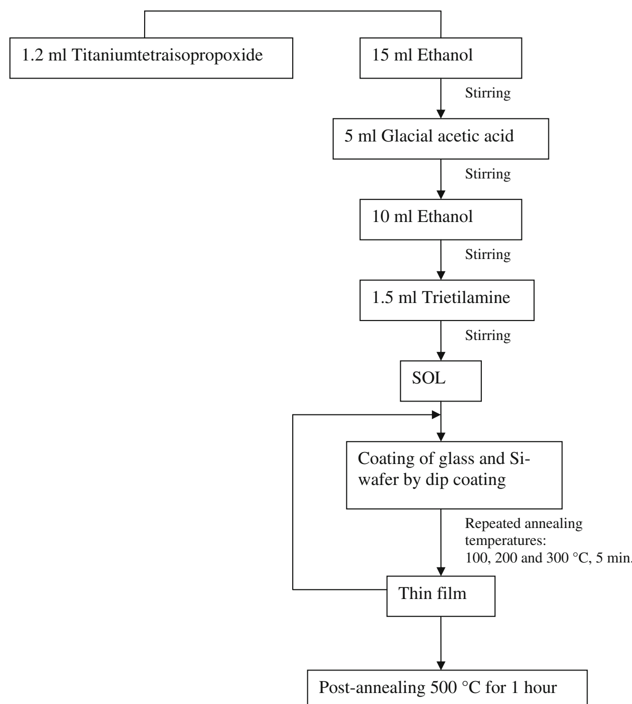

Fig. 1 The flowchart diagram of the sol–gel process for the preparation of TiO_2 thin films on the glass and Si wafer

After each dipping process, samples were left to repeated annealing processes at 100, 200, and 300 °C. Finally, all the samples were post-annealed at a fixed temperature of 500 °C for 1 h period.

In order to obtain a rectifying contact on front p-Si surface with TiO_2 coating high-purity aluminium was coated in high-vacuum under the pressure of 10^{-7} Torr. The structure of Al/TiO_2/p-Si/Al (MIS) structure is given in Fig. 2.

X-ray powder diffraction (XRD) measurements of TiO_2 thin film on glass was performed at room temperature by the Rigaku D/MAX-2200 with Cu*Kα*-radiation unit. The UV–VIS transmittance measurements of TiO_2 thin films on the microscope glass were performed with Shimadzu UV-3600 in the spectral range of 300–1,100 nm. AFM, the surface morphology of TiO_2 thin films on the microscope glass was observed using a SPM Solver-PRO (NT-MDT) in

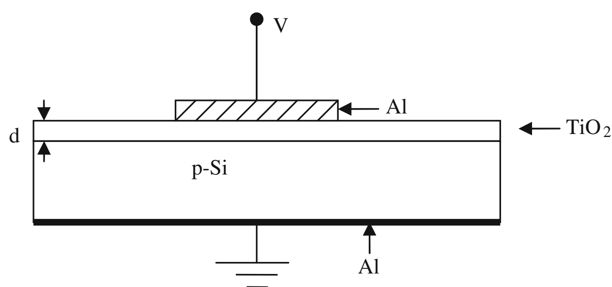

Fig. 2 Schematic diagram of Al/TiO_2/p-Si (MIS) structure

semi contact mode. The images were recorded with a resolution of 128 × 128 points per line on a 1 × 1 μm area using commercial Si cantilevers NSG 10 series with the Au conductive coating, with a nominal elasticity constant $K_N = 11.5$ N/m. The forward and reversable bias capacitance–voltage (*C*–*V*) and conductance–voltage (*G*–*V*) measurements were performed at 1 MHz by using a HP 4192 A LF impedance analyzer (5 Hz–13 MHz) and the test signal of 50 m V_{rms}. All measurements were carried out at room temperature and in the dark.

Results and discussion

XRD patterns of TiO_2 thin films on the microscope glass with 5 and 10 layers in Fig. 3 shows obvious peaks. The TiO_2 films exhibits (101), (004), and (020) peaks of anatase structure [12]. The anatase (101) peak is expected at $2\theta = 24°$. The crystallite size of these samples was calculated from X-ray line broadening by means of the Scherrer Formula [13],

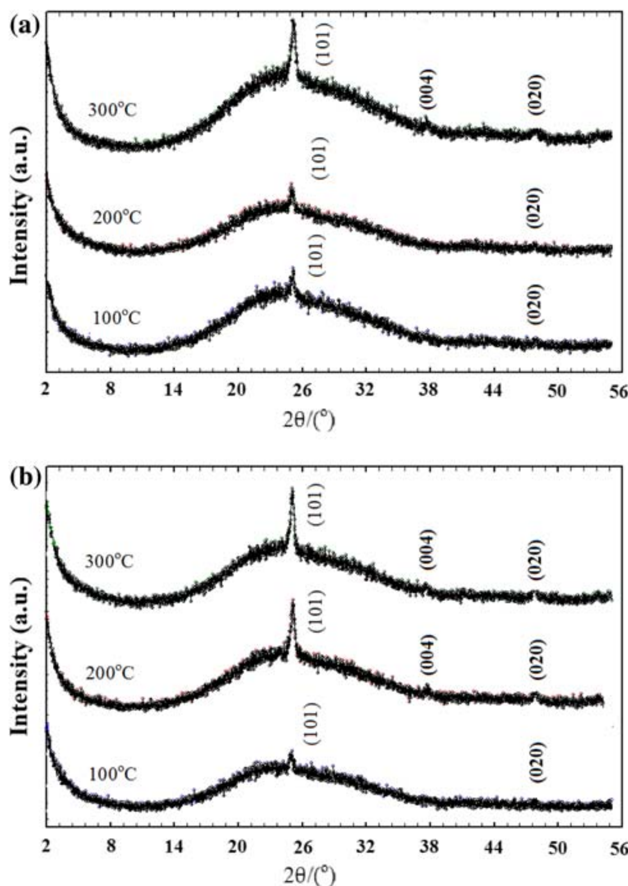

Fig. 3 XRD patterns (**a**) 5 layer and (**b**) 10 layer of TiO_2 thin film on the glass

$$d = \frac{0.9\lambda}{\beta \cos\theta}, \quad (1)$$

where λ, θ, and β were the X-ray wavelength, the Bragg angle, and the integral breadth of reflection located at 2θ full width to half maximum, respectively. The crystallite sizes are given in Table 1. It was observed that the average crystallite size increases with the increasing number of layers and decreasing repeated annealing temperatures. The X-ray results were compared with the results in the literature [12]. Similar results like (i) the films consist of TiO_2 phase and (ii) the orientation of the crystallite with the annealed temperature were obtained.

The *AFM* images of TiO_2 thin films on the microscope glass, in three dimensions, having 1×1 $(\mu m)^2$ area, are exhibited in Figs. 4 and 5. It was observed that average grain size values of the TiO_2 thin films increased with the increasing number of layer and decreasing repeated annealing temperature. Furthermore, average roughness values of thin TiO_2 films decreases with the increasing number of layer and decreasing repeated annealing temperature. The *AFM* images TiO_2 are compared with the published results [14, 15]. There are some differences in the surface roughness of the films. These differences were also attributed to the film preparation method, design of apparatus, used solution, and its molaritites.

Figure 6 show the *UV–VIS* spectra of TiO_2 thin films on the microscope glass for different repeated annealing temperatures, in wavelength range of 300–1,100 nm. This region was the transparent region of the films. In the transparent region a minimum for normal incidence of the impinging light was given by $T_{min} = 4n_f^2 n_s/(n_f^2 + n_s)^2$ where n_f and n_s are the index of refractions of the film and substrate, respectively. The value of n_f can be deduced for the wavelength at the minimum of transmission. If n_f is known the pattern of transmisson in the transparent region with successive minima and maxima can be used in order to evaluate the thickness of the TiO_2 films. The thickness of the layer can be calculated from two maxima or two minima by means of the equation [16]

$$d = M\lambda_1\lambda_2/2[(\lambda_1 n_f(\lambda_2) - \lambda_2 n_f(\lambda_1))], \quad (2)$$

where M, n_f (λ_1), and n_f (λ_2) are the number of oscillations between the two extrema occurring at λ_1, λ_2, and the corresponding refractive indices, respectively. Usually in this region n_f is nearly constant: $n_f \approx n_f(\lambda_1) = n_f(\lambda_2)$ and the value of $n_f(\approx 2)$ can be deduced from he wavelength at the minimum of transmission (T_{min})

$$n_f = \{[n_s(2 - T_{min}) + 2n_s(1 - T_{min})^{1/2}]/T_{min}\}^{1/2}, \quad (3)$$

Figure 7 shows the TiO_2 thin film thickness versus repeated annealing temperature. It can be seen that the thickness of TiO_2 thin films decreases with the increase in

Table 1 Crystallite size, grain size, and roughness parameters of TiO_2 thin films on the glass

Sample number	Number of layers	Repeated annealing temperature (°C) (5 min)	Post-annealing temperature (°C) (1 h)	Average crystallite size (nm)	Average grain size (nm)	Average roughness (nm)
ND1	5	100	500	24.2	55	2.22
ND2	10	100	500	38.3	82	1.15
ND3	5	200	500	17.2	49	4.05
ND4	10	200	500	21.4	53	1.63
ND5	5	300	500	11.4	49	4.25
ND6	10	300	500	15.2	51	1.82

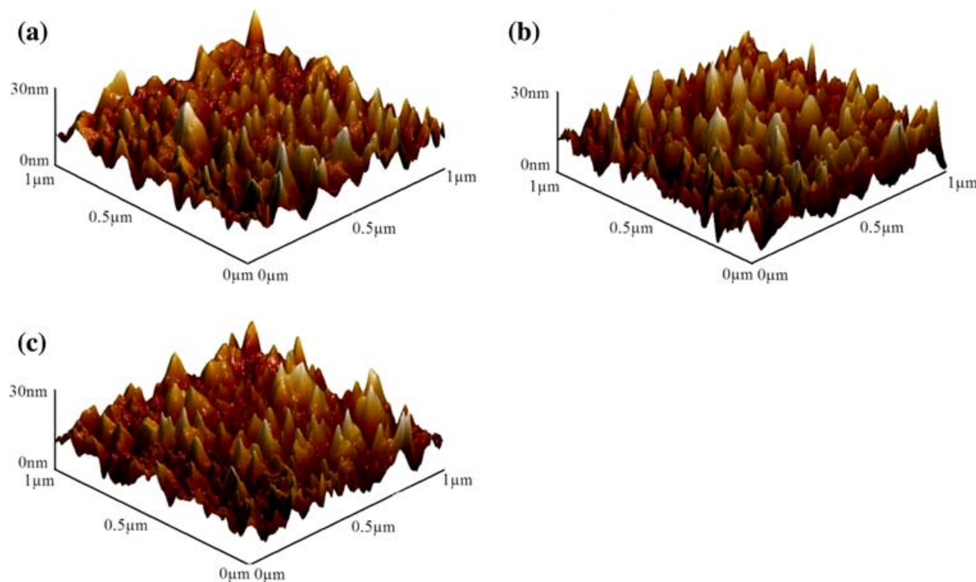

Fig. 4 The surface images of 5 layer TiO_2 thin films taken by atomic force microscope (AFM) (**a**) ND1; (**b**) ND3; and (**c**) ND5

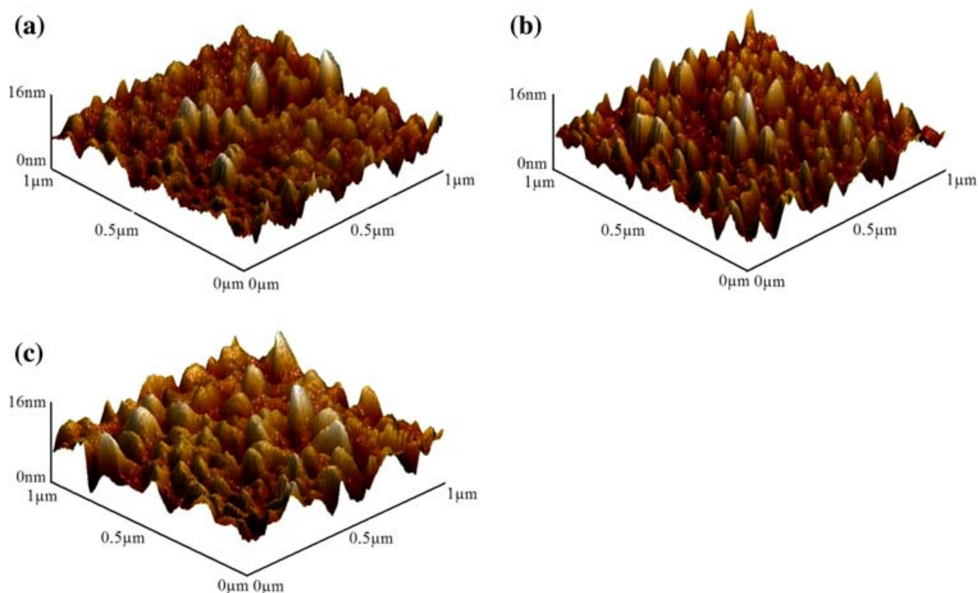

Fig. 5 The surface images of 10 layer TiO_2 thin films taken by atomic force microscope (AFM) (**a**) ND2; (**b**) ND4; and (**c**) ND6

the repeated annealing temperature and decrease in the number of layers. The optical band gap of TiO_2 thin films has also been determined by means of UV–VIS transmission measurements as shown in Fig. 6. For this the fundamental absorption coefficient (α) was evaluated using the equation $\alpha = (\ln T^{-1})/d$ where d is the film thickness

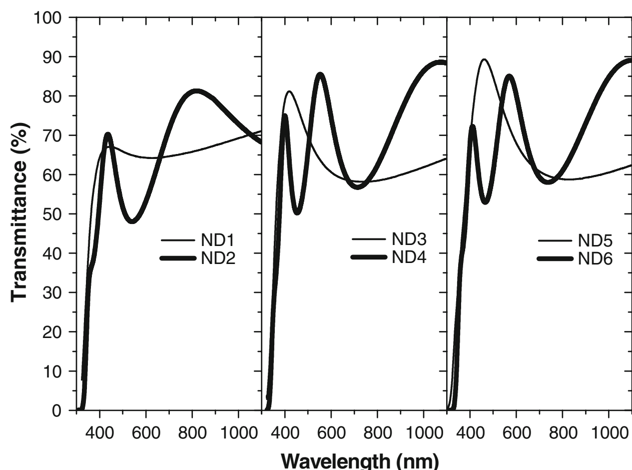

Fig. 6 The transmittance spectra of TiO_2 thin films prepared at various repeated annealing temperatures and number of layers

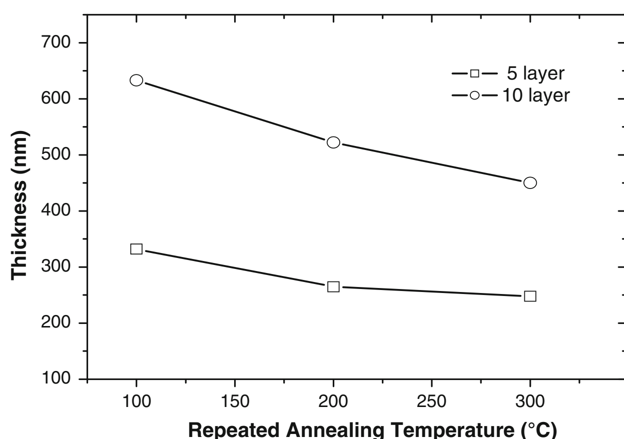

Fig. 7 The thickness of 5 and 10 layer TiO_2 thin films on the glass versus repeated annealing temperature

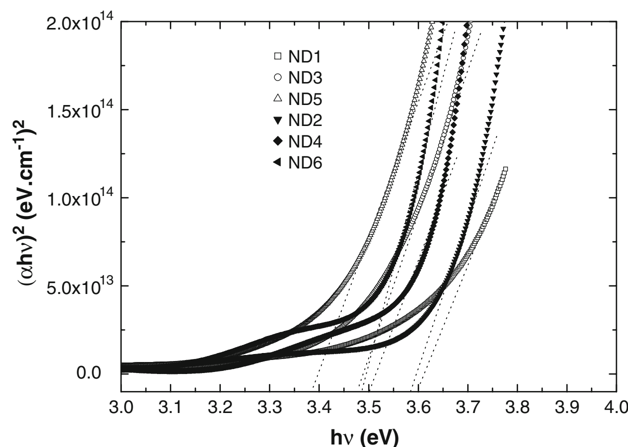

Fig. 8 The plots of $\alpha h\nu$ versus $h\nu$ curves of 5 and 10 layer TiO_2 films on the glass

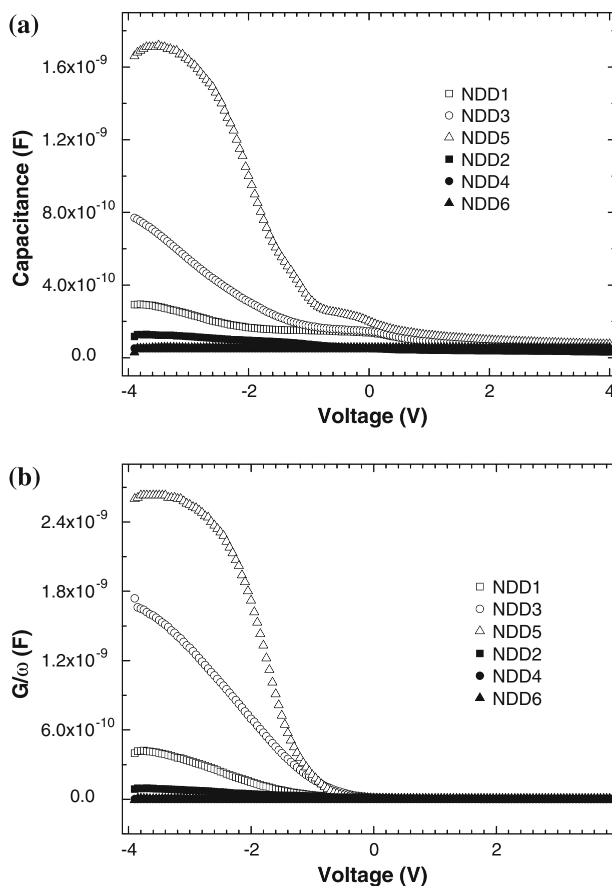

Fig. 9 The voltage dependent plots of the high-frequency (1 MHz) (**a**) capacitance and (**b**) conductance curves of Al/TiO_2/p-Si (MIS) structure at room temperature

and T is the transmittance. Figure 8 shows the variation of $(\alpha h\nu)^2$ versus $h\nu$ for all the films. The nature of the plots indicates the existence of direct optical transitions. The band gap (E_g) is determined by extrapolating the straight line portion of the plot to the energy axis. In Fig. 6, it is easy to observe that the direct energy band gaps range from 3.38 to 3.59 eV. The band gap energy (E_g) values of the films obtained at different deposition temperatures lie in the range of 3.00–3.80 eV [17–20], which is quite comparable with the reported values. These differences were also attributed to the film preparation method and annealed temperature.

The series resistance (R_s) is an important parameter for MIS structure. When a voltage is applied across the MIS structure, the series resistance of the structure will share applied voltage. In this study, the values of the series resistance (R_s) was evaluated from the reverse and forward bias C–V and G/ω–V data at the high-frequency (1 MHz) using the method developed by Nicollian and Goetzberger [21]. The C–V and G/ω–V plots of Al/TiO_2/p-Si (MIS) structure, obtained in the voltage range of −4 V to +4 V,

Table 2 Various parameters obtained from C–V (1 MHz) characteristics of Al/TiO_2/p-Si (MIS) structures at room temperature

Sample number	Number of layers	Insulator layer (Repeated annealing temperature and time)	Insulator layer (Post-annealing temperature and time)	C_{ox} (F/cm^2)	R_S (Ω)
NDD1	5	100 °C, 5 min	500 °C, 1 h	2.88×10^{-10}	292
NDD2	10	100 °C, 5 min	500 °C, 1 h	7.19×10^{-10}	561
NDD3	5	200 °C, 5 min	500 °C, 1 h	1.71×10^{-9}	201
NDD4	10	200 °C, 5 min	500 °C, 1 h	1.26×10^{-10}	357
NDD5	5	300 °C, 5 min	500 °C, 1 h	5.14×10^{-11}	95
NDD6	10	300 °C, 5 min	500 °C, 1 h	5.27×10^{-11}	223

are given in Fig. 9a and b, respectively. As seen from Fig. 9a and b both curves have three distinct regimes of accumulation–depletion–inversion. When the MIS structure is biased in to strong accumulation, the impedance ($Z_{ma} = 1/Y_{ma}$) is given by [21]

$$Z_{ma} = \frac{1}{G_{ma} + j\omega C_{ma}}, \quad (4)$$

where C_{ma} and G_{ma} are the measured capacitance and conductance, in strong accumulation region. Series resistance is the real part of the impedance ($Z_{ma} = 1/Y_{ma}$) or:

$$R_S = \frac{G_{ma}}{G_{ma}^2 + (\omega C_{ma})^2}, \quad (5)$$

The insulator layer capacitance (C_{ox}) is obtained by substituting R_s from Eq. 5 into relations

$$C_{ox} = C_{ma}\left[1 + \left(\frac{G_{ma}}{\omega C_{ma}}\right)^2\right] = \frac{\varepsilon_i \varepsilon_0 A}{d}, \quad (6)$$

The effect of interface states can be eliminated when the C–V and G/ω–V plots are obtained at high-frequency ($f \geq 500$ kHz) [22], since interface states (N_{ss}) cannot follow ac signal. In this case, the R_s seems to be the most important parameter which causes the main electrical parameters (C, G) of MIS structure. As seen from Table 2, the values of R_s decreases with increasing repeated annealing temperatures and decreasing insulator layer. In addition the values of C_{ox} decreases with increasing number of layer.

Conclusions

The X-ray diffraction patterns, atomic force microscope (*AFM*) images, and *UV–VIS* spectra showed that crystallinity in TiO_2 thin films were significantly affected by repeated annealing temperature. It was observed that the average crystallite size and average grain size of TiO_2 films were decreased with increasing repeated annealing temperature. On the other hand, the average crystallite size and average grain size of TiO_2 films were increased with increasing number of layer. Furthermore, average roughness values of thin TiO_2 film decreases with the increasing number of layer and decreasing repeated annealing temperature. The values of R_s of Al/TiO_2/p-Si (MIS) structures decreases with increasing repeated annealing temperatures and decreasing insulator layer. In addition the values of C_{ox} decreases with increasing number of layer. It was concluded that the repeated annealing temperature should be controlled at 300 °C in order to grow TiO_2 thin films with good crystallite and optical quality.

Acknowledgements This work is supported by Ankara University (BIYEP) Project number 2005-K-120-140-8 and Ankara University Scientific Research Project (BAP), 2007-07-45-054.

References

1. Kannan K, Balasubrahmaniyam R (1988) Thin Solid Films 109:59
2. Yang L, Scott Saavedra S, Armstrong NR, Hayes J (1994) Anal Chem 66:1254
3. Ito S, Kitamura S, Yanagia S (2003) Solar Energy Mater Solar Cells 76:3
4. Czapla A, Kusior E, Bucko M (1989) Thin Solid Films 182:15
5. Sanon G, Rup R, Mansingh A (1990) Thin Solid Films 190:287
6. Zhang JY, Boyd IW, Sullivan BJ, Kelly PK, Seneteur JP (2002) J Non-Cryst Solids 303:134
7. Chatelon JP, Terrier C, Bernstein E, Berjoan R, Roger JA (1994) Thin Solid Films 247:162
8. Maddalena A, Dal Maschio R, Dire S, Raccanelli A (1990) J Non-Cryst Solids 121:365
9. Choi Y, Yamamoto S, Umebayashi T, Yoshikawa M (2004) Solid State Ionics 172:105
10. Tracey SM, Hodgson SNB, Ray AK, Ghassemlooy Z (1998) J Mater Process Technol 77:86
11. Kern W (1993) Handbook of semiconductor cleaning technology Noyes, New York
12. Yu J, Zhao X, Zhao Q (2000) J Mater Sci Lett 19:1015
13. Cullity BD (1978) Elements of X-ray diffraction, 2nd edn. Addison-Wesley, California, USA
14. Leprince-Wang Y, Yu-Zhang K (2001) Surf Coat Technol 140:155
15. Yang W, Marino J, Monson A, Wolden CA (2006) Semicond Sci Technol 21:1573
16. Svanepoel R (1983) J Phys E Sci Instrum 16:1214

17. Tang H, Berger H, Schmid PE, Levy F, Burri G (1993) Solid State Commun 87:847
18. Pascaul J, Camassel J, Mathieu H (1978) Phys Rev B 18:5606
19. Wang S, Xia G, Shao J, Fan Z (2006) J Alloys Compd 424:304
20. Park YR, Jim KJ (2005) Thin Solid Films 484:34
21. Nicollian EH, Brews HR (1982) Metal-oxide semiconductor (MOS) physics and technology. Wiley, New York
22. Nicollian EH, Brews HR (1967) Bell Syst Technol J 46:1055